Opt Quant Electron (2008) 40:431–437
DOI 10.1007/s11082-008-9223-8

A comparison of optical modulator structures using a matrix simulation approach

Kjersti Kleven · Scott T. Dunham

Received: 1 September 2007 / Accepted: 20 May 2008 / Published online: 10 June 2008
© Springer Science+Business Media, LLC. 2008

Abstract The high operating frequency, small dimensions and complex nature of advanced integrated photonics structures lead to a need for full 3D simulations in order to obtain accurate propagation characteristics. However, 3D simulations are very computationally expensive, especially for design optimization. Therefore a matrix analysis has been employed to model the propagation characteristics and analyze structure variations without the need to perform a separate simulation for each design iteration. Designs investigated include two that are promising for silicon-based integrated dense wavelength division multiplexing applications: the resonant cavity modulator and the microring resonator. The ability to accurately model and quickly optimize these electro-optic devices will be important for future large-scale integrated optics systems.

Keywords Numerical simulation · Silicon photonics · Integrated optics

1 Introduction

Future integrated optics applications will require modulators that have a fast, strong response, narrow linewidth and large modulation depth in a compact structure. The Mach-Zehnder modulator structure has been the most commonly used layout to achieve high-speed, low drive voltage modulators, but the large device dimensions, often greater than 1 mm, required to achieve the necessary modulation depth requires investigation of alternative structures that can meet both the transmission and size requirements (Liu et al. 2007). Two such structures that have the potential to achieve this are the Fabry-Perot type resonant cavity modulator (Kleven-McLauchlan and Dunham 2006) and the microring resonator modulator. The modeling of both of these structures however, requires 3D full-wave simulation in order to accurately capture the propagation characteristics. Since a typical device will be greater than 20 μm in length, and for the microring resonator, at least 20 μm in width as well, a full

K. Kleven (✉) · S. T. Dunham
Department of Electrical Engineering, University of Washington, Seattle, WA 98195-2500, USA
e-mail: kkleven@ee.washington.edu

3D simulation of the entire structure would be extremely lengthy, and separate simulations would be required for each design variation. This analysis therefore uses a matrix modeling approach to significantly reduce the computational resources necessary to perform 3D analysis, which is critical for device design and optimization. The matrix modeling method is then applied to the resonator structures described above for investigation of the applicability of both structures to dense wavelength division multiplexing (DWDM) applications.

2 Resonator structures

This work considers the simulation of two resonator structures: the Fabry-Perot type resonant cavity and the microring resonator. For the resonant cavity structure, a Bragg grating is created using a series of appropriately spaced circular holes on each side of a cavity region, which has a length designed to obtain the desired resonant wavelength, as illustrated in Fig. 1. There is a sharp transmission peak at the resonant wavelength and very little throughput off resonance due to constructive/destructive interference within the structure. Changing the index of refraction of the cavity region causes a change in the propagation constant in that region, which shifts the resonant wavelength and provides modulation at the detected wavelength.

The microring resonator is a circular waveguide side-coupled to one or more straight waveguides, as shown in Fig. 2. The path length around the ring determines the resonant wavelength as only certain wavelengths continue propagating in the ring and the rest are coupled back into the straight waveguide. The resulting transmission spectrum will be either stopband (thru port in Fig. 2) or passband shaped (drop port in Fig. 2).

A deep resonance can be achieved if the critical coupling conditions are met (Niehusmann et al. 2004). Changing the propagation constant of the light in the ring waveguide can change

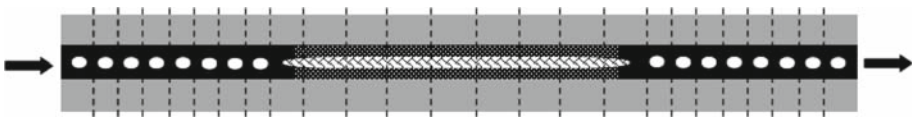

Fig. 1 Resonant cavity modulator with holes forming the Bragg grating (white), a p-type silicon waveguide (black), and a slot waveguide cavity region with n-type silicon and an EO polymer (white hashed). The arrows indicate input and output of light and the simulation sections (dashed lines) are shown for reference

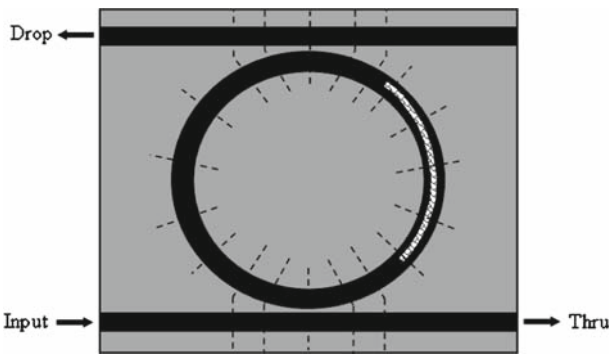

Fig. 2 Microring resonator modulator on SOI with silicon (black) and EO polymer (white hashed) in a hybrid slot waveguide, with the simulation sections indicated by dashed lines. The arrows indicate light transmission

the resonant wavelength and allow for modulation around a fixed wavelength with this structure.

A change in the index of refraction of silicon can be achieved through the free carrier dispersion effect, and though this can achieve sufficient index variation, it is a relatively slow effect. Another option for achieving the index change is to incorporate an EO polymer material into the design, which exhibits a change in index of refraction with an applied field. Using a hybrid silicon/EO polymer slot waveguide enhances the effectiveness of the polymer index variation since the field in this TE-like mode is confined primarily to the lower index polymer region rather than the silicon ridges on either side (Almeida et al. 2004). Both types of modulation schemes have been investigated in this work.

3 Simulation and analysis

The descriptions of the devices above highlight the need to very accurately simulate the propagation characteristics, losses and coupling within the structures in order to accurately predict the transmission spectrum. Because full wave simulation is so computationally expensive, this work uses a matrix approach to model the transmission characteristics (Lu et al. 2006; Hall et al. 1988). With this approach small, unique sections of the device can be simulated individually, with the full, 3D propagation of the fields being simulated and then analyzed at each port to determine the throughput, reflection and loss of the section. The transmission and propagation characteristics of each section are then used to determine the transmission spectrum and resulting device characteristics.

The matrix analysis used for this work divides the structure into a number of small sections, each of which contains the field propagation characteristics, as described above, and categorizes the input and output of each section as either an internal boundary or an external input/output, as outlined in Glock et al. (2002), and repeated sections (Fig. 2) need only be simulated once. In this way, the coupling of the light propagation in the ring waveguide and the straight waveguide is included, even though the ring waveguide does not have external inputs/outputs so that, for a two-port structure, the overall inputs (a) are related to the overall outputs (b) through:

$$\begin{bmatrix} b_1 \\ b_2 \end{bmatrix} = \begin{bmatrix} S_{11} & S_{12} \\ S_{21} & S_{22} \end{bmatrix} \begin{bmatrix} a_1 \\ a_2 \end{bmatrix} \tag{1}$$

The scattering matrix (S_i) of each section is then incorporated into a diagonal matrix ($\mathbf{S}_{\mathrm{Tot}}$) of scattering parameters ordered from external input to external output:

$$\mathbf{S}_{Tot} = \begin{bmatrix} S_1 & 0 & 0 \\ 0 & S_n & 0 \\ 0 & 0 & S_{N_{tot}} \end{bmatrix} \tag{2}$$

Next two permutation matrices are created: one that separates the internal and external boundaries ($\mathbf{M}_{Int}$) and the other that specifies an internal output at one boundary as the internal input at the next boundary ($\mathbf{M}_{Bnd}$), which for the ring resonator, provides the necessary coupling between the microring and the straight waveguide. This yields the final transmission matrix ($\mathbf{T}$), with the following relationship between internal boundaries and external ports:

$$\begin{bmatrix} \mathbf{a}_{Int} \\ \mathbf{b}_{Ext} \end{bmatrix} = \mathbf{M}_{Bnd}\mathbf{S}_{Tot}\mathbf{M}_{Int} = \begin{bmatrix} \mathbf{T}_{11} & \mathbf{T}_{12} \\ \mathbf{T}_{21} & \mathbf{T}_{22} \end{bmatrix} \begin{bmatrix} \mathbf{a}_{Int} \\ \mathbf{a}_{Ext} \end{bmatrix} \tag{3}$$

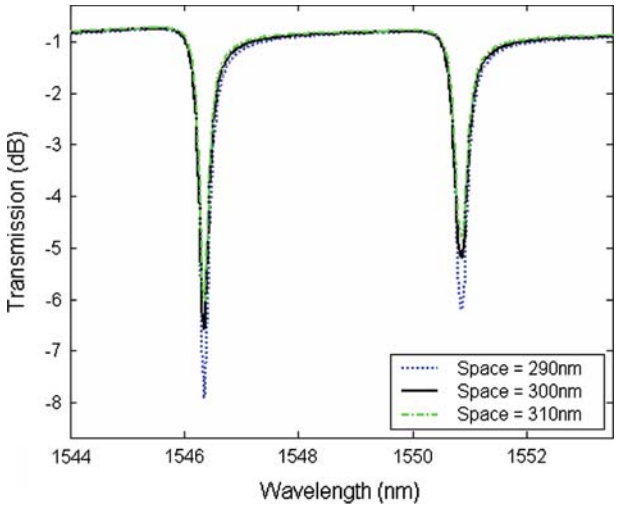

Fig. 3 The transmission through a straight waveguide with a side-coupled ring waveguide showing that variations in the gap spacing can result in variations in the depth of extinction from −7.9 dB for 290 nm to −6.2 dB for 310 nm at 1546.4 nm

Since the primary interest is in the transmission characteristics at external inputs/outputs, eliminating the internal boundaries results in the final transmission equation for the full structure:

$$\mathbf{b}_{Ext} = \left[\mathbf{T}_{21}\left(\mathbf{1} - \mathbf{T}_{11}\right)^{-1}\mathbf{T}_{12} + \mathbf{T}_{22}\right]\mathbf{a}_{Ext} \tag{4}$$

The simulation times for the coupling sections are longer than single waveguide sections since it is important to have regions large enough to capture the mode coupling, though there is still a dramatic savings in computational time over simulating the entire structure.

The transmission matrix modeling method is used to analyze both a resonant cavity and a microring resonator modulator. The primary objectives considered in this analysis are the dimensions, throughput, full-width at half-maximum (FWHM) of the resonant linewidth and the modulation depth, which relates the difference in transmission at a fixed wavelength due to a change in propagation constant.

One of the important aspects of a microring resonator design is the coupling coefficient, which affects the FWHM, throughput and modulation depth. The coupling coefficient for a microring resonator will be determined by the distance between the straight waveguide and the ring waveguide. The tight tolerances of the gap spacing may be a challenge for large-scale incorporation of microring ring resonators into integrated optics applications, since a variation on the order of 10 nm can cause a significant variation in the extinction ratio of the resonator, as illustrated in Fig. 3 for the transmission spectrum of the TM-like mode with a 300 ± 10 nm spacing between the ring waveguide and straight waveguide.

The resonant cavity modulator structure considered here has 600×250 nm silicon waveguides with twelve 100 nm-diameter holes spaced 505 nm apart in each Bragg grating and a slot waveguide in the cavity region with a 100×250nm polymer region and 250×250 nm silicon ridges on each side. The microring resonator has silicon waveguides of the same dimensions side-coupled to a 30 µm diameter ring waveguide. Modulation is simulated by incorporating a 25 µm length of active material (either silicon with $\Delta n = 0.003$ or an EO polymer slot waveguide with $V_a = 2V$) within the ring waveguide.

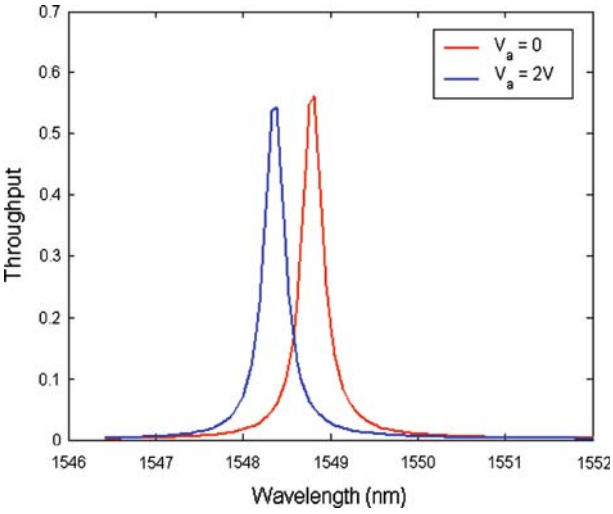

Fig. 4 Throughput of the resonant cavity modulator with a hybrid slot waveguide in the cavity region

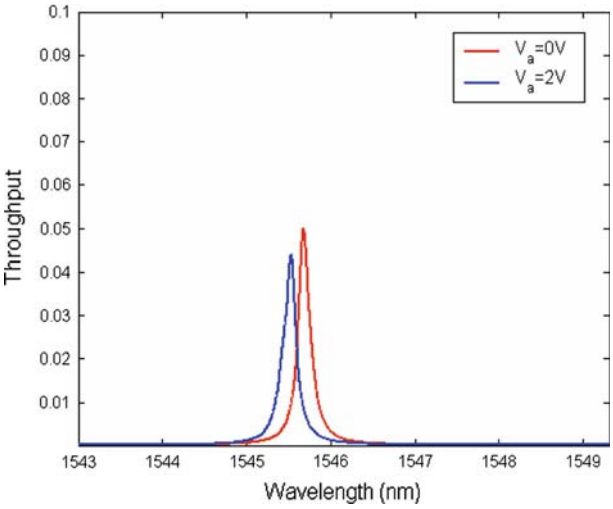

Fig. 5 Throughput at the drop port of a microring resonator modulator with a hybrid slot waveguide included in a section of the ring waveguide

The resulting transmission peak of a TE-like mode has a FWHM of 0.29 nm, a maximum throughput of 0.57 at the resonant wavelength, and a modulation depth of 89% in a device that is 40 µm in length from input grating edge to output grating edge, as illustrated in Fig. 4.

The TE-like mode of a microring structure similar to that illustrated in Fig. 2 results in very little throughput at the drop port, yet it still has a FWHM of 0.18 nm and a modulation depth of 78%, as illustrated in Fig. 5. Improving the design of the coupling regions should increase the transmission at the drop port to take advantage of the narrow linewidth of this structure and including a hybrid slot waveguide in the other half of the ring would enhance the modulation depth.

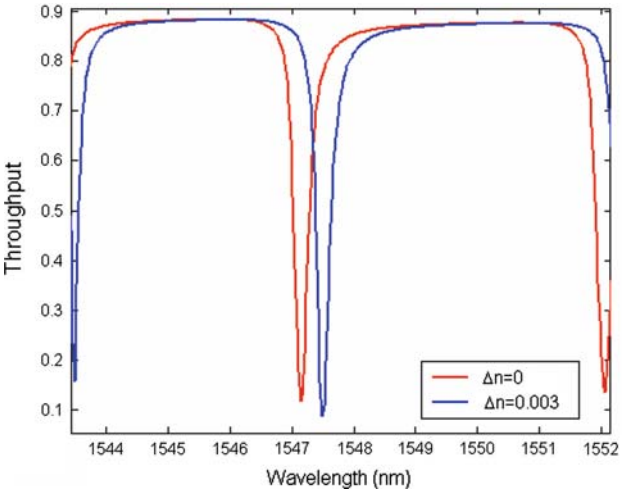

Fig. 6 A large modulation depth is achieved at the thru port with this 30 μm diameter ring resonator incorporating an active silicon section in the ring waveguide

A TM-like mode of a silicon microring resonator modulator with a single side-coupled waveguide has a FWHM of 0.23 nm, minimum and maximum throughput of 0.12 and 0.88, respectively, and modulation depth of 83%, as illustrated in Fig. 6, which is similar to the resonant cavity device, but the 30×30 μm footprint would be much larger.

4 Conclusion

Both of the structures investigated in this work can achieve the required design parameters of optical modulators for future integrated optics applications, though the hybrid slot microring resonator has the potential to meet the tight requirements of future integrated DWDM applications. Recognizing the periodicity in the device structures and using transmission matrices significantly reduces the required analysis time and provides a fast, efficient simulation approach that could be used for investigation and optimization of many integrated optics devices.

References

Almeida, V.R., Xu, Q., Barrios, C.A., Lipson, M.: Guiding and confining light in void nanostructures. Opt. Lett. **29**, 1209–1211 (2004)

Glock, H.W., Rothemund, K., van Rienen, U.: CSC—a procedure for coupled S-parameter calculations. IEEE Trans. Magn. **38**, 1173–1176 (2002)

Hall, R.C., Mittra, R., Mitzner, K.M.: Analysis of multilayered periodic structures using generalized scattering matrix theory. IEEE Trans. Antenna Prop. **36**, 511–516 (1988)

Kleven-McLauchlan, K., Dunham, S.T.: Analysis of a compact modulator incorporating a hybrid silicon/electro-optic polymer waveguide. IEEE J Select Topics Quantum Electron **12**, 1455–1460 (2006)

Liu, A., Liao, L., Rubin, D., Nguyen, H., Ciftcioglu, B., Chetrit, Y., Izhaky, N., Paniccia, M.: High-speed optical modulation based on carrier depletion in a silicon waveguide. Opt. Express **15**, 660–668 (2007)

Lu, Q.Y., Guo, W.H., Phelan, R., Byrne, D., Donegan, J.F., Lambkin, P., Corbett, B.: Analysis of slot characteristics in slotted single-mode semiconductor lasers using the 2-D scattering matrix method. IEEE Photon. Technol. Lett. **18**, 2605–2607 (2006)

Niehusmann, J., Vorckel, A., Bolivar, P.H., Wahlbrink, T., Henschel, W., Kurz, H.: Ultrahigh-quality-factor silicon-on-insulator microring resonator. Opt. Lett. **29**, 2861–2863 (2004)

Copyright of Optical & Quantum Electronics is the property of Springer Science & Business Media B.V. and its content may not be copied or emailed to multiple sites or posted to a listserv without the copyright holder's express written permission. However, users may print, download, or email articles for individual use.